

## Medial prefrontal cortex lesions disrupt prepotent action selection signals in dorsomedial striatum

### Highlights

- Medial prefrontal cortex (mPFC) lesions alter stop-signal performance
- mPFC lesioned rats perform better on STOP trials but worse on GO trials
- Directional firing in dorsomedial striatum (DMS) is altered in mPFC lesioned rats

### Authors

Adam T. Brockett,  
Stephen S. Tennyson,  
Coreylyn A. deBettencourt,  
Madeline Kallmyer, Matthew R. Roesch

### Correspondence

brockett@umd.edu (A.T.B.),  
mroesch@umd.edu (M.R.R.)

### In brief

Here, Brockett et al. show that lesions to medial prefrontal cortex (mPFC) disrupt action initiation but not the inhibition or adaptation of action plans on a variant of the stop-signal task. Moreover, Brockett et al. show that lesions to mPFC alter directional signaling in dorsomedial striatum.



## Article

# Medial prefrontal cortex lesions disrupt prepotent action selection signals in dorsomedial striatum

Adam T. Brockett,<sup>1,2,3,\*</sup> Stephen S. Tennyson,<sup>1,2</sup> Corelyn A. deBettencourt,<sup>1,2</sup> Madeline Kallmyer,<sup>1,2</sup> and Matthew R. Roesch<sup>1,2,4,5,\*</sup>

<sup>1</sup>Department of Psychology, University of Maryland, College Park, MD 20742, USA

<sup>2</sup>Program in Neuroscience and Cognitive Science, University of Maryland, College Park, MD 20742, USA

<sup>3</sup>Twitter: @adam\_brockett

<sup>4</sup>Twitter: @MattRoesch\_UMD

<sup>5</sup>Lead contact

\*Correspondence: brockett@umd.edu (A.T.B.), mroesch@umd.edu (M.R.R.)

<https://doi.org/10.1016/j.cub.2022.06.025>

## SUMMARY

The ability to inhibit or adapt unwanted actions or movements is a critical feature of almost all forms of behavior. Many have attributed this ability to frontal brain areas such as the anterior cingulate cortex (ACC) and the medial prefrontal cortex (mPFC), but the exact contribution of each brain region is often debated because their functions are not examined in animals performing the same task. Recently, we have shown that ACC signals a need for cognitive control and is crucial for the adaptation of action selection signals in dorsomedial striatum (DMS) in rats performing a stop-change task. Here, we show that unlike ACC, the prelimbic region of mPFC does not disrupt the inhibition or adaption of an action plan at either the level of behavior or downstream firing in DMS. Instead, lesions to mPFC correlate with changes in DMS signals involved in action initiation and disrupt performance on GO trials while improving performance on STOP trials.

## INTRODUCTION

Cognitive control is a behavioral mechanism that facilitates the adaption and reshaping of motor outputs in a manner consistent with internal goals.<sup>1–7</sup> Research aimed at understanding the neural systems supporting cognitive control have predominantly focused on frontal brain areas, such as anterior cingulate cortex (ACC) and medial prefrontal cortex (mPFC), and their role(s) in the instantiation of control<sup>1–9</sup> as well as striatal brain regions, such as dorsomedial striatum (DMS) and motor cortex, for their role(s) in representing planned actions.<sup>5,7,10–12</sup> Despite being identified as contributing to the implementation of control, the exact role of individual frontal brain regions in this process is often debated.<sup>13</sup>

The stop-signal task is a classic behavioral paradigm that has been used to study cognitive control.<sup>14</sup> Successful performance on the stop-signal task requires subjects to refrain from making a habitual, often directional response, on a minority of trials, when a cue (i.e., a STOP cue) is presented unexpectedly. Research using a novel-variant of the stop-signal task where rats were required to initiate a response in one direction, only to then redirect their response in the opposite direction when a STOP cue was presented (i.e., stop-change tasks), has shown task-related activity in both ACC<sup>15</sup> and mPFC<sup>16</sup> and that unilateral lesions of ACC impairs inhibitory control.<sup>17</sup> Although a role for ACC in inhibitory control has long been theorized,<sup>2,18</sup> other work investigating task-switching behaviors has implicated mPFC in supporting the inhibition and redirection of behavior as well.<sup>1,4,12,19–29</sup> Similarities

in neural correlates and proposed functions raise the possibility that mPFC and ACC may have overlapping functions in governing behavior and downstream targets. This overlap is further compounded by controversy surrounding whether there are discrete boundaries between these regions in the rodent brain.<sup>13</sup>

To explore the degree of functional overlap between mPFC and ACC in the rodent brain, we performed unilateral lesions of mPFC (prelimbic) in both male and female rats performing our stop-change task while recording downstream of the same hemisphere of DMS. We chose DMS based on previous evidence showing that DMS generates robust action signals that correlate with the rats intended movement.<sup>17,30</sup> Using these response-selective signals as a guide, we hypothesized that lesions to mPFC would disrupt action selection and impair behavioral performance on STOP trials. Instead, we found that mPFC lesions reduced accuracy on GO trials, improved accuracy on STOP trials, and slowed behavior overall. Consistent with these behavioral changes, action selection signals in DMS were weaker and slower to emerge. Collectively, our results suggest that mPFC contributes to the drive to initiate an initial action but that unlike ACC, mPFC does not appear to be responsible for the inhibition of an inappropriate response.

## RESULTS

In order to establish a role for mPFC in stop-signal performance, we performed unilateral excitotoxic lesions of mPFC and recorded



from DMS in the same hemisphere in both male and female rats. Unilateral lesions were chosen to minimize the impact on behavior and to reduce the potential recruitment of redundant systems that might support task performance.<sup>31–33</sup> Rats were randomly assigned to treatment groups (control,  $n = 7$ ; lesion,  $n = 6$ ), and no differences in the percentage of correct trials ( $t(11) = 0.6247$ ,  $p = 0.5449$ ) or the number of trials performed ( $t(11) = 0.9431$ ,  $p = 0.3659$ ) were detected between the groups prior to surgery.

### mPFC lesions impair and improve performance on GO trials and STOP trials, respectively

The structure of the behavioral task is presented in Figures 1A and 1B. On one wall of each recording chamber, a central port was located above two adjacent fluid wells. Each trial began with the illumination of house lights that instructed the rat to nose poke into the central port. After 1 s, a directional cue was flashed for 100 ms on either the rats right or left side. On 80% of trials (GO trials), presentation of this directional cue instructed the rat to exit the port and respond in the direction of the light to receive a small ( $\sim 70 \mu\text{L}$ ) liquid sucrose reward. On the remaining 20% of trials (STOP trials), the initial sequence of events was identical; however, a second directional cue was illuminated in the opposite direction 0–100 ms after the rat exited the port. During STOP trials, rats had to adapt their behavior and respond in the direction of the second light to receive reward.

Unilateral lesions of mPFC (Figure 1C) worsened and improved performance on both GO and STOP trials, respectively (Figure 1D). A two-way ANOVA across sessions revealed significant main effects for treatment ( $F(1,1494) = 12.95$ ,  $p = 0.0003$ ) and trial type ( $F(1,1494) = 365.3$ ,  $p < 0.0001$ ), as well as a significant interaction (treatment by trial type) ( $F(1,1494) = 75.82$ ,  $p < 0.0001$ ). Bonferroni-corrected post hoc comparisons revealed lesioned rats performed significantly worse on GO trials (control,  $78.71 \pm 0.40$ ; lesion,  $75.60 \pm 0.59$  [mean  $\pm$  SEM];  $t(1,494) = 3.613$ ,  $p = 0.0019$ ) and performed significantly better on STOP trials (control,  $61.80 \pm 0.60$ ; lesion,  $69.28 \pm 0.82$  [mean  $\pm$  SEM];  $t(1,494) = 8.702$ ,  $p < 0.0001$ ; see Figure S2A for breakdown by hemisphere).

One underlying premise of the stop-signal task is that subjects build up an automatic tendency to respond quickly to the first cue, making stopping more difficult and subjects more cautious following a STOP trial (i.e., conflict adaptation).<sup>6,7,14,15,17,34,35</sup> To investigate whether mPFC lesions altered this canonical phenomenon, we examined the effect of the previous trial type on performance of GO and STOP trials, respectively (Figure 1E). We conducted a three-way ANOVA comparing the percentage of correct trials across previous (i.e., g or s) and current trial type (i.e., G or S). We observed significant main effects for current trial type ( $F(1,2983) = 523.5$ ,  $p < 0.0001$ ), previous trial type ( $F(1,2983) = 25.09$ ,  $p < 0.0001$ ), and treatment ( $F(1,2983) = 5.519$ ,  $p = 0.0189$ ), as well as significant interactions for previous trial type by current trial type ( $F(1,2983) = 5.519$ ,  $p = 0.0189$ ) and for current trial type by treatment ( $F(1,2983) = 77.77$ ,  $p < 0.0001$ ). Bonferroni-corrected post hoc comparisons revealed mPFC lesioned rats were significantly worse on GO trials and significantly better on STOP trials, regardless of the preceding trial identity (all  $p < 0.05$ ). Notably, there was no previous trial type by treatment interaction ( $F(1,2983) = 3.505$ ,  $p = 0.0613$ ) or previous trial type by current trial type by treatment interaction ( $F(1,2983) = 0.2029$ ,  $p = 0.6524$ ), indicating the previous trial

influences behavior the same for both control and lesion groups. Finally, we did not observe differences in the total number of rewarded trials ( $t(747) = 1.496$ ,  $p = 0.1350$ ), the number trials that were omitted ( $t(747) = 0.9326$ ,  $p = 0.3513$ ), or the overall number of errors made across all trials ( $t(747) = 1.442$ ,  $p = 0.1496$ ) as a function of treatment (Figure S1).

### mPFC lesions slow movement times on both GO and STOP trials

Improved performance on STOP trials might result from weaker reactions to the first cue and/or slower movements to the fluid well to allow for better detection of the second cue. To test this, we investigated whether lesions altered reaction times (i.e., time from the first cue light turning on to the time required to leave the central port) and movement times (i.e., the time from leaving the central port to the time the well was entered).

For reaction times, we collapsed across trial type because this behavioral measure preceded the onset of the STOP cue. mPFC lesions significantly slowed reaction times (control,  $0.316 \pm 0.007$  s; lesion,  $0.349 \pm 0.007$  [mean  $\pm$  SEM];  $t(747) = 3.117$ ,  $p = 0.0019$ ) (Figure 1F). Notably, lesioned rats exhibited significant slowing to the first cue on trials that followed a STOP trial. In a two-way ANOVA comparing reaction times, we observed a main effect for treatment ( $F(1,1494) = 22.08$ ,  $p < 0.0001$ ) and previous trial type ( $F(1,1494) = 36.99$ ,  $p < 0.0001$ ); however, there was no significant interaction between treatment and previous trial type ( $F(1,1494) = 0.5815$ ,  $p = 0.4458$ ), indicating that although lesioned rats reacted slower to the first cue in general, adjustments as a consequence to trial sequence did not differ from controls.

For movement times, we observed significant main effects for treatment ( $F(1,1494) = 62.50$ ,  $p < 0.0001$ ) and trial type ( $F(1,1494) = 568.3$ ,  $p < 0.0001$ ), as well as a significant interaction (treatment  $\times$  trial type) ( $F(1,1494) = 4.005$ ,  $p = 0.0456$ ) (Figure 1G). Bonferroni-corrected pairwise comparisons revealed that lesioned rats were slower on both GO (control,  $0.511 \text{ s} \pm 0.01$ ; lesion,  $0.586 \text{ s} \pm 0.01$  [mean  $\pm$  SEM];  $t(1,494) = 7.005$ ,  $p < 0.0001$ ) and STOP (control,  $0.708 \pm 0.01$ ; lesion,  $0.753 \pm 0.01$  [mean  $\pm$  SEM];  $t(1,494) = 4.175$ ,  $p = 0.0002$ ) trials. Notably, there was also a significant interaction between treatment and trial type ( $F(1,1494) = 4.005$ ,  $p = 0.0456$ ), with slowing of GO trials in lesioned rats being more prominent than slowing on STOP trials (see Figure S2A for breakdown by hemisphere).

We then examined movement time as a function of trial history (Figure 1H). The three-way ANOVA revealed main effects of current trial type ( $F(1,2973) = 958.8$ ,  $p < 0.0001$ ) and treatment ( $F(1,2973) = 74.95$ ,  $p < 0.0001$ ), but no significant effect for previous trial type ( $F(1,2973) = 0.1367$ ,  $p = 0.7116$ ) or any significant interactions ( $p > 0.05$ ), confirming that lesioned rats performed slower overall, regardless of trial type, and that the influence of the previous trial type did not differ between groups.

Finally, we asked whether both control and lesioned rats exhibited a speed-accuracy tradeoff on STOP trials. We plotted the percentage of correct STOP trials as a function of movement time on STOP trials and performed a linear regression analysis. Although both control and lesioned rats exhibited a significant positive correlation (suggesting that as rats slowed, their behavior their accuracy on STOP trials improved), the strength of this relationship was significantly weaker in lesioned rats (Fisher  $r$ -to- $z$  transform,  $Z = 4.24$ ,  $p < 0.001$ ) (Figure S1).

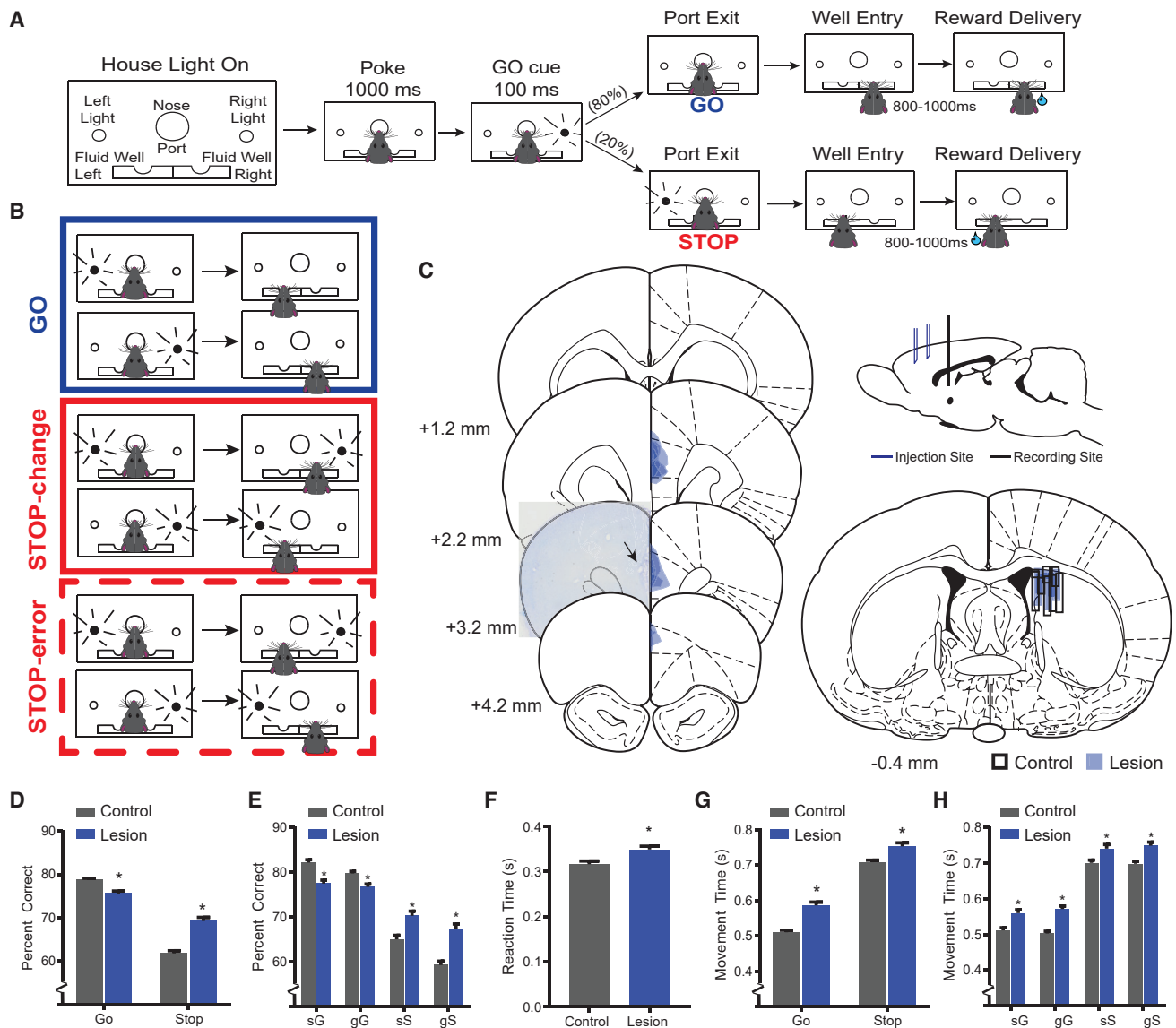


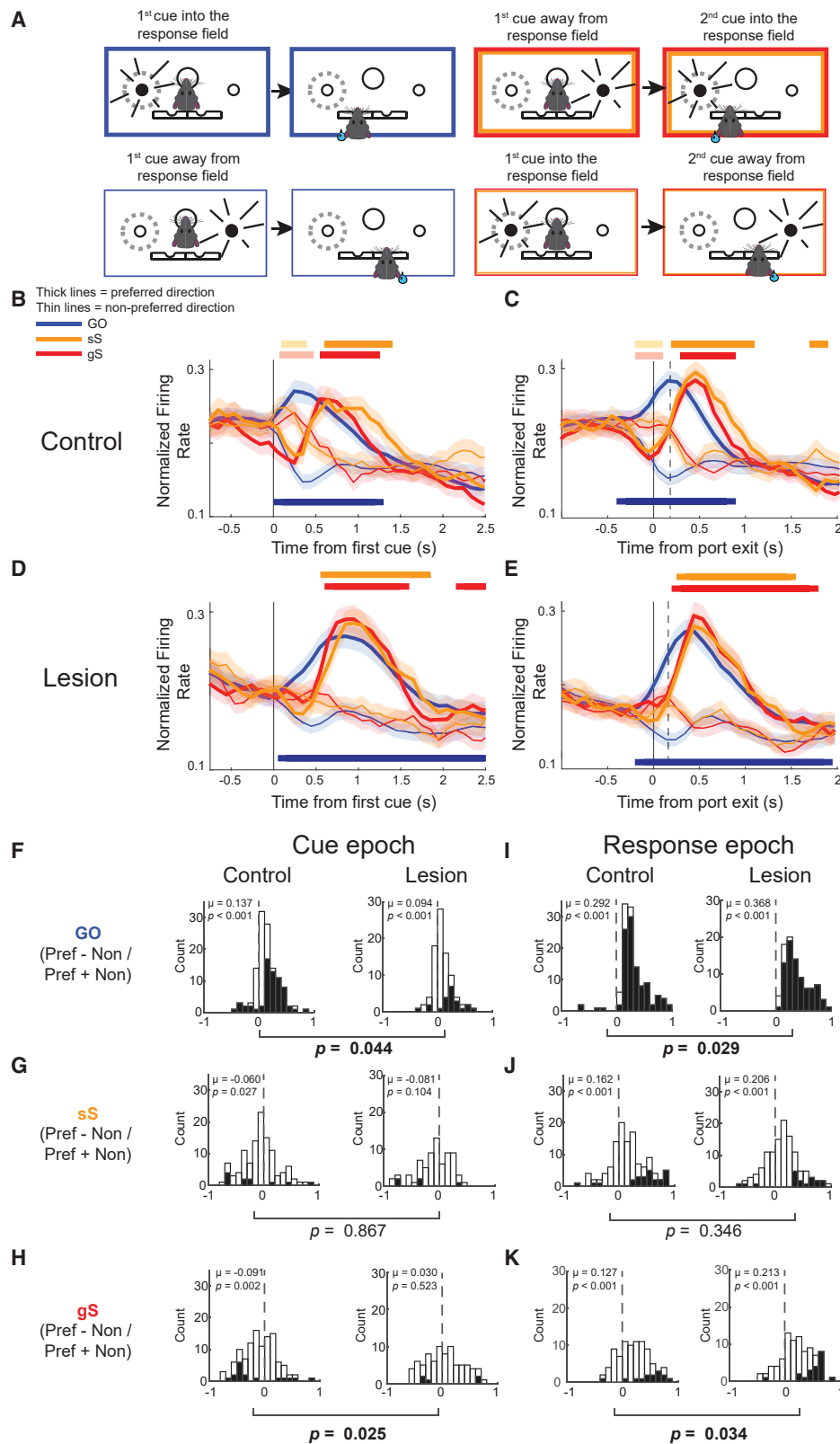
**Figure 1. Task design and behavioral analysis**

(A) Schematic of stop-change task. Following the house lights, rats made a nose poke for 1,000 ms before a light cue was illuminated on either the right or left side. On 80% of trials (GO trials), this light corresponded to the correct direction that the rat needed to move to receive reward. On 20% of trials, a second light was illuminated after the initial GO cue directing the rat to inhibit their initial response to the first cue in favor of making a response in the direction of the second cue. (B) Illustration of GO (blue), STOP (red), and STOP-error (dashed red) trial types. (C) Schematic of lesion placements (left) and electrode placements (bottom right) in the prelimbic part of mPFC and DMS. Photomicrograph overlaid over lesion schematic (left) shows Nissl-stained section of mPFC with a representative lesion (black arrow). (D) Percent correct for control and lesioned animals on GO and STOP trials. (E) Percent correct data for sequence effects: gG, go, go; sG, stop, go; sG, stop, go; and sS, stop, stop. (F) Reaction time data plotted as a function of treatment group. (G) Movement time data for both GO and STOP trials. (H) Movement time data for sequence effects comparing control and lesioned animals. For (D)–(H), error bars represent  $\pm$  SEM over recording sessions. Asterisk (\*) represents comparisons between control and lesion, all Bonferroni adjusted  $p < 0.05$ . See also [Figures S1](#) and [S2](#).

**mPFC lesions attenuate and enhance direction selectivity before and after initiation of the behavioral response, respectively**

Previously, we have shown that activity in both mPFC and DMS reflects response direction and is negatively correlated with

movement time.<sup>16,30</sup> In line with this, we hypothesized that if mPFC played a role in the biasing of action selection via DMS, then directional signals would be delayed and/or diminished in mPFC lesioned rats. Importantly, our lesion manipulations were not specific to DMS-projecting neurons only.



(legend on next page)

To explore this possibility, we examined firing for all directionally selective DMS neurons in control ( $n = 155$ ) and lesioned ( $n = 102$ ) rats. Directional selectivity was defined as significantly different firing between the two directions during the response epoch (port exit to fluid well entry; Wilcoxon;  $p < 0.05$ ) collapse across all correct trials (Figure 2A; examples of single units can be seen in Figures S3A and S3B).<sup>15–17,30,34–36</sup> Based on a waveform analysis, the overwhelming majority of these cells were classified as medium spiny neurons (MSNs), and only  $\sim 4\%$  in controls and  $\sim 2\%$  in lesioned animals were classified as fast-spiking interneurons (FSIs), in line with our previous work and the work of others<sup>30,37–39</sup> (see Figures S5A and S5B split into MSN and FSI).

Average firing over all directional neurons for both control and lesioned rats is displayed in Figures 2B–E. Thick and thin lines represent firing when responses were made correctly into (i.e., preferred direction) or away from (i.e., non-preferred direction) the response field of each neuron, respectively (Figure 2A). “Preferred direction” was defined by the response direction that elicited the strongest firing averaged across all correct trials during the response epoch. We observed no significant differences in raw average baseline firing rates (control,  $9.875 \pm 0.901$  spk/s; lesion,  $8.421 \pm 0.835$  spk/s;  $Z = 0.3388$ ,  $p = 0.7348$ ), nor for task-related firing rate averaged over all correct trial types (control,  $10.23 \pm 0.830$  spk/s; lesion,  $9.313 \pm 1.132$  spk/s [mean  $\pm$  SEM];  $Z = 0.8550$ ,  $p = 0.3925$ ).

In Figure 2, trials are aligned to the presentation of the first cue light (Figures 2B and 2D) and response initiation (center port exit) (Figures 2C and 2E), which are common events between GO (blue) and STOP trials. STOP trials are broken down into gS (red) and sS (orange) (Figure 2A). Tick marks above the lines represent significant differences between the two response directions for each trial type (i.e., difference between thick and thin lines; sliding t test every 100 ms,  $p < 0.05$ ).

In controls, directional signals emerged quickly after the onset of the first cue light for GO (blue), sS (orange), and gS (red) trials (Figure 2B). As seen by the color-coded bars above and below the population histogram, selectivity became significant within the first 100 ms for GO and gS trials and within the first 200 ms for sS trials. The slower development of directional selectivity is consistent with the behavioral finding that rats were better on sS trials compared with gS trials.<sup>6,7,15,17,30,34,36</sup> When examining population activity aligned to response initiation (i.e., center port exit) in Figure 2C, we observed that on GO trials, directional selectivity

continued to remain significant until the completion of the response. On STOP trials, directional selectivity flipped at the time of the stop-change reaction time (SCRT; the difference in the average movement time on correct STOP and GO trials), reflecting the direction of the second cue (i.e., the STOP cue).

Average firing over time for directional units in the DMS of mPFC lesioned rats is illustrated in Figures 2D and 2E. Activity showed reduced selectivity to the first cue light during both GO and STOP trials (i.e., both sS and gS trial types) (Figure 2D). On GO trials, directional selectivity did not become significant until 200 ms after onset of the first cue light, and on STOP trials, activity never significantly reflected the direction of the first cue light like it did for controls (sliding t test analysis over 100 ms time bins; pale red and orange ticks;  $p < 0.05$ ). Only after center port exit (Figure 2E) did accurate directional signals emerge on STOP trials in rats with mPFC lesions (dark red and orange ticks).

To quantify these results over all neurons within these populations, we calculated directional selectivity by subtracting firing for correct movements away from each cell’s response field (non-preferred direction) from firing for correct movements to be made into the response field (preferred direction) divided by the sum (preferred – non-preferred/preferred + non-preferred; for distributions examining raw firing rate, see Figure S4). Within control rats, we observed a significant positive shift in the overall distribution of single units on GO trials (Wilcoxon signed-rank test,  $\mu = 0.137$ ,  $p < 0.001$ ) (Figure 2F). The same was true for lesions as well (Wilcoxon signed-rank test,  $\mu = 0.094$ ,  $p < 0.001$ ); however, direct comparison of the firing distributions of all neurons from control and lesioned rats revealed that this shift was larger in controls (Wilcoxon rank-sum test,  $Z = 2.001$ ,  $p = 0.044$ ) (Figure 2F). Further, within lesioned rats, sS and gS distributions were not significantly shifted in either direction (Wilcoxon signed-rank test; sS,  $\mu = -0.081$ ,  $p = 0.104$ ; gS,  $\mu = 0.030$ ,  $p = 0.523$ ) (Figures 2G and 2H). This suggests that in mPFC lesioned rats, DMS neurons did not exhibit the initial selectivity in firing for the first cue (Figure 1D). Direct comparison of directional index distributions during the cue epoch for control and lesioned rats showed that firing of DMS neurons exhibited a stronger shift in controls on gS trials (Wilcoxon rank-sum test,  $Z = -2.472$ ,  $p = 0.246$ ) (Figure 2H). Although significantly shifted in controls, and not in lesions, on sS trials, the two distributions were not significantly different from each other (Wilcoxon rank-sum test,  $Z = -0.166$ ,  $p = 0.8677$ ). Thus, lesions appeared to more strongly impact firing on gS trials, consistent with behavior (Figure 2G).

### Figure 2. mPFC lesions impair the emergence of response-selective signals in DMS to the first cue

(A) Illustration of preferred (thick lines) and non-preferred (thin lines) directions for GO (blue) and STOP (sS, orange; gS, red) trials. (B and C) Population histograms for the first cue epoch (B) and response epoch (C) for control rats ( $n = 155$  cells). Blue lines represent normalized firing on GO trials (i.e., no conflict trials). Orange lines represent normalized firing on correct sS trials (i.e., conflict trials when a STOP trial precedes another STOP trial) and red lines represent normalized firing on gS trials (i.e., high conflict trials when a GO precedes a STOP trial). Thick and thin lines represent firing in either the preferred (thick) or non-preferred (thin) direction. Ribbons represent SEM. Boxes above the graph follow the same color code and indicated significant differences between preferred and non-preferred directions (sliding t tests,  $p < 0.05$ ). (D and E) Population histograms for the first cue epoch (D) and response epoch (E) for mPFC lesioned rats ( $n = 102$  cells). Color code mirrors the code used for controls. (F–K) Single unit distributions for the first cue epoch (F–H) and response epoch (I–K) for GO (F and I, blue), sS (G and J, orange), and gS (H and K, red) trials for control and mPFC lesioned rats. Black bars indicate neurons with a significant difference between directions (Wilcoxon signed-rank test,  $p < 0.05$ ). Brackets with p values below each chart reflect direct comparison between control and lesion distributions for each measure (Wilcoxon rank-sum test). Note: all Wilcoxon tests are performed on the entire distribution and not just on significant cells (i.e., black bars). See also Figures S3–S5.



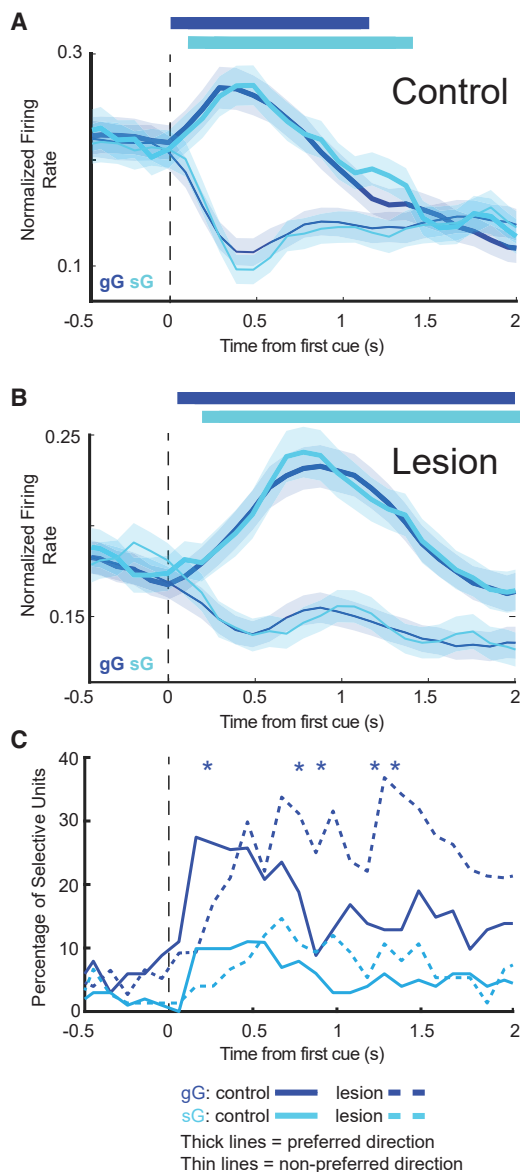


**Figure 3. mPFC lesions delay the emergence of directional selective signals on gG and sG trials**

(A) Population histogram comparing firing on gG (dark blue) and sG (light blue) trials for control rats. Thick and thin lines represent firing in either the preferred (thick) or non-preferred (thin) direction. Ribbons represent SEM. Boxes above the graph follow the same color code and indicated significant differences between preferred and non-preferred directions (sliding t tests,  $p < 0.05$ ).

(B) Population histogram comparing firing on gG (dark blue) and sG (light blue) trials for lesioned rats. Color code mirrors the code used for controls.

(C) Chi-square analysis comparing the percentage of significantly selective units during the first cue epoch for gG trials (royal blue lines) and sG (sky blue lines) trials. Control rats are represented with solid lines. Lesion rats are represented by dashed lines. Asterisk (\*) indicates statistical difference between controls and lesions ( $p < 0.05$ ; chi-square).

When directly comparing directional index distributions across treatment during the response epoch, we found that for GO trials, distributions of DMS neurons were similarly shifted in the positive direction for both control and lesioned rats (Wilcoxon

signed-rank test; control,  $\mu = 0.292$ ,  $p < 0.001$ ; lesion,  $\mu = 0.368$ ,  $p < 0.001$ ), with the distribution of directional indices being significantly more strongly shifted in lesions possibly reflecting compensatory firing after stalled initiation (Wilcoxon rank-sum test,  $Z = -2.186$ ,  $p = 0.029$ ) (Figure 2I). Similarly, for STOP trials, entire directional distributions of DMS neurons were shifted in the positive direction for both controls and lesions, with stronger shifts again being observed in lesions, however, only significantly for gS trials (gS, Wilcoxon rank-sum test,  $Z = -2.126$ ,  $p = 0.0335$ ; sS, Wilcoxon rank-sum test,  $Z = -0.942$ ,  $p = 0.3460$ ) (Figures 2J and 2K).

### Firing of DMS neurons reflects the response direction on GOs earlier in controls

To better understand the failure of DMS neurons to encode the first cue, we examined the time course of when population and single units became selective on GO trials. The frequency of GO trials (~80% of all trials) is thought to induce behaviorally reflexive responding to the presentation of the first directional cue, resulting in increased accuracy and a gradual speeding of responding.<sup>6,7,14,15,17,34–36,40,41</sup> We have shown that in DMS neurons, directional selectivity is stronger to the first cue in control rats (Figure 2F). Here, we split GO trials by the previous trial type to determine whether mPFC lesions differentially impact the firing of DMS neurons on gG (i.e., GO trials that were preceded by a GO trial) and sG (i.e., GO trials that were preceded by a STOP trial) (Figure 3).

Figures 3A and 3B illustrate average firing aligned to first cue onset for gG (royal blue) and sG (teal) trials for control and lesioned rats. Consistent with the results described above for GO trials collapsed across sG and gG trials (Figures 2B–2E), directional selectivity emerged later in DMS neurons in lesioned rats for both gG and sG trial types. However, for both groups, directional selectivity of DMS neurons emerged earlier on gG trials compared with sG trials, mirroring behavioral performance (i.e., rats were faster and more accurate on gG compared with sG trials) (Figures 3A and 3B). These results suggest that although mPFC lesions reduced the appearance of first cue selectivity in DMS neurons overall, the role of mPFC in enhancing directional selectivity in DMS neurons to the first cue in DMS based on trial sequence is unaffected.

To quantify these effects in single neurons, we performed a sliding chi-square analysis comparing the percentage of significantly selective units over 100 ms time bins between control and lesions on gG and sG trials, respectively. Selective units were determined by performing a Wilcoxon rank-sum test comparing firing between non-preferred and preferred direction for cells from control and lesioned rats, for each 100 ms bin. Consistent with our findings in Figure 2, on gG trials, the frequency with which we observed significantly selective units from the total number of units observed in controls was greater than the frequency observed in lesioned rats in the 200 ms after the first cue compared with lesioned rats (chi-square,  $p < 0.05$ ) (Figure 3C, blue lines). On sG trials, we observed a similar pattern, where controls exhibited a greater frequency of selective units from the total number of units observed within the 300 ms after the first cue compared with DMS neurons in lesioned animals, although this was not significant (chi-square,  $p > 0.05$ ) (Figure 3C, teal lines). Thus, significantly more

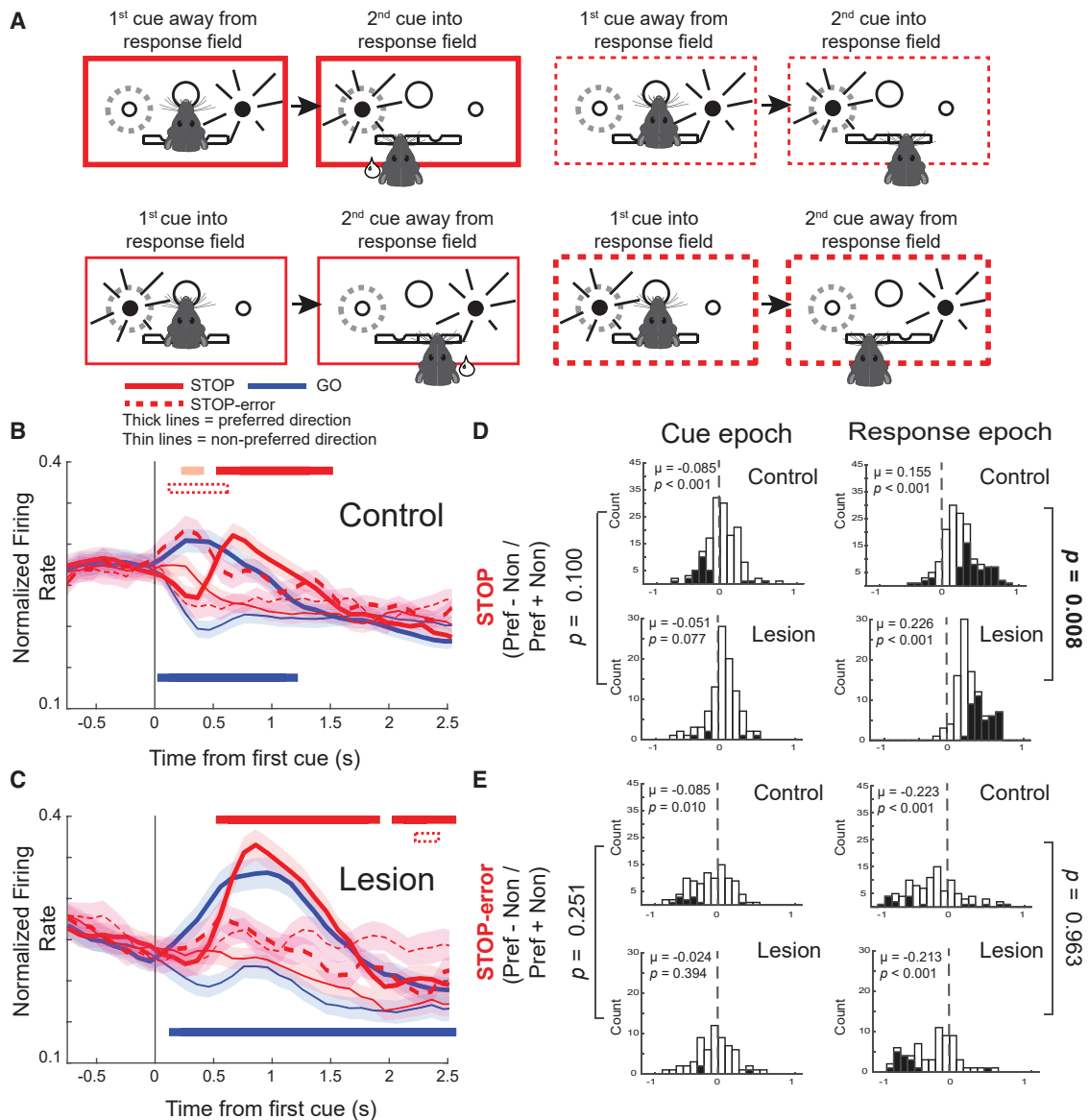


**Figure 4. Neural activity reflected the incorrect direction on STOP-error trials**

(A) Illustration of STOP (solid red line) and STOP-error (red-dashed line) trial types.

(B) Population histograms for control rats ( $n = 155$  cells) during the first cue epoch. Solid red lines represent normalized firing on correct STOP trials and the red-dashed lines represent normalized firing on STOP-error trials. Thick and thin lines represent firing in either the preferred (thick) or non-preferred (thin) direction. Ribbons represent SEM. Boxes above/below the graph follow the same color code and indicate significant differences between preferred and non-preferred directions (sliding t tests every 100 ms,  $p < 0.05$ ).

(C) Population histograms for mPFC lesioned rats ( $n = 102$  cells) during the first cue epoch. Color code mirrors the code used for controls.

(D and E) Distributions of single units for control and lesioned rats during the cue and response epochs for correct (D) and STOP-error (E) trials. Black bars indicate individual cells that were significantly shifted from 0 (Wilcoxon signed-rank test,  $p < 0.05$ ). Brackets indicated p values where direct comparison between control and lesioned rats were performed (Wilcoxon rank-sum test).

neurons encoded information about the first cue earlier in controls compared with lesions. Collectively, [Figures 2 and 3](#) show that when the directional selectivity of DMS neurons over time is examined in multiple ways, across two behaviorally relevant epochs, single units in the DMS of lesioned animals show a reduction in selectivity to the first cue that correlates with behavioral performance.

**Neural activity reflected the incorrect direction on STOP-error trials**

To explore whether mPFC lesions alter firing on STOP-error trials, we plotted the average firing over all directional neurons, aligned to first cue onset, for control and lesion rats during correct and errant STOP trials in [Figures 4A–4C](#). Thick and thin lines represent firing when responses were made into (i.e., preferred



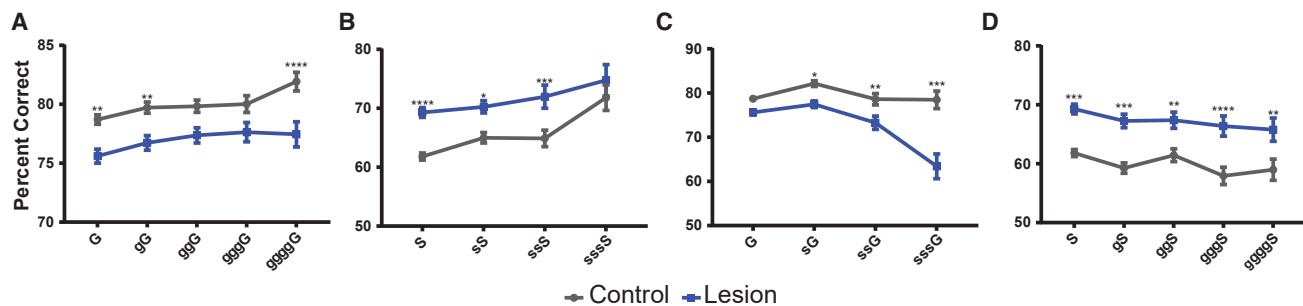


**Figure 5. mPFC lesions do not impair conflict adaptation or development of automaticity**

Percent correct measures on a current GO or STOP trial (“G” or “S,” respectively) as a function of the number of preceding GO or STOP trials (“g” or “s,” respectively) for (A) gG trials, (B) sS trials, (C) sG trials, and (D) gS trials. For all graphs, error bars represent  $\pm$  SEM. Stars represent significant Bonferroni adjusted *p* values for comparisons between controls and mPFC lesioned rats ( $p < 0.05$ ). Control data are presented in grey, and lesion data are presented in blue.

direction) or away from (i.e., non-preferred direction) the response field of each neuron, respectively. Thus, thick lines on error trials (dashed) represent when the first cue was in the response field, and the rats made a response in that direction, although the STOP cue signaled for the movement to be made in the opposite direction (i.e., away from the response field). As above, tick marks above the lines represent significant differences between the two response directions (i.e., difference between thick and thin lines; sliding *t* test every 100 ms,  $p < 0.05$ ).

In controls, on correct STOP trials (red solid lines), directional selectivity of DMS neurons reflecting the direction of the first cue (pale red tick marks) was followed by encoding of the second cue (Figure 4B). In contrast, on STOP-error trials, population firing reflected the direction of the first cue but failed to signal the correct direction indicated by the second cue (Figure 4B). Unlike controls, directional selectivity did not develop to the first cue on correct trials and only ever reflected the direction of the second cue later in the trial in lesioned rats (Figure 4C, dark red ticks).

To further quantify the directional signal across the population and at the level of single neurons, we computed directional indices (preferred – non-preferred/preferred + non-preferred) for STOP-correct and STOP-error trials for each neuron using the average firing rate for the first cue epoch and the response epoch (Figures 4D and 4E). In controls, on correct STOP trials, the distribution of directional indices was significantly shifted in the negative and positive direction during the first cue epoch (Wilcoxon signed-rank test,  $\mu = -0.085$ ,  $p < 0.001$ ) and the response epoch (Wilcoxon signed-rank test,  $\mu = 0.155$ ,  $p < 0.001$ ), respectively, indicating that the firing of most neurons reflected the direction of the first cue, followed by the direction of the second cue, consistent with accurate encoding on STOP trials (Figure 4D). As seen in the sS and gS results described above in Figures 2G and 2H, directional index distributions during the first cue epoch were not significantly shifted during the first cue epoch (Wilcoxon signed-rank test,  $\mu = -0.051$ ,  $p = 0.077$ ) and were more strongly shifted in the positive direction compared with lesioned rats during the response epoch (Wilcoxon rank-sum test,  $Z = -2.659$ ,  $p = 0.008$ ) (Figure 4D). Thus, the activity of fewer and more DMS neurons represented the direction of the first and second cue, respectively, in lesions compared with controls.

Consistent with the hypothesis that direction was miscoded during stop-error trials, during the response epoch, both control and lesion distributions were shifted in the negative direction reflecting the direction of the first, not the second cue (Wilcoxon rank-sum test,  $Z = 0.047$ ,  $p = 0.963$ ) (Figure 4E). Further, on error trials, the distribution of directional indices was significantly shifted in the negative direction during the first cue epoch in controls (Wilcoxon signed-rank test,  $\mu = -0.065$ ,  $p = 0.010$ ), but not in lesions (Wilcoxon signed-rank test,  $\mu = -0.024$ ,  $p = 0.394$ ), although the two distributions were not significantly different from each other (Wilcoxon rank-sum test,  $Z = 1.147$ ,  $p = 0.251$ ).

#### mPFC lesions leave trial sequence effects intact

Previously, we have seen improvement in accuracy when rats were presented with strings of back-to-back trials of the same identity (i.e., rats are better at sssS trials compared with sS trials and worse at gggS trials compared with gS trials).<sup>36</sup> For both GO and STOP trials, respectively, we asked whether the number of preceding GO trials or STOP trials altered accuracy (Figures 5A–5D). The current trial is presented as either “G” (GO) or “S” (STOP), and the number of preceding trials is indicated by the number of lowercase “g’s” or “s’s” in front of the current trial type. Given the low percentage of STOP trials, we were unable to reliably look at trials that contained more than three STOP trials in a row or four GO trials in a row.

For gG and sS trials, we observed significant main effects for treatment (gG,  $F(1,3711) = 50.56$ ,  $p < 0.0001$ ; sS,  $F(1,2509) = 33.11$ ,  $p < 0.0001$ ) and number of preceding GO/STOP trials (gG,  $F(4,3711) = 3.616$ ,  $p = 0.0060$ ; sS,  $F(3,2509) = 8.867$ ,  $p < 0.0001$ ), but no significant interaction (treatment by number of preceding GO/STOPs) (gG,  $F(4,3711) = 0.7373$ ,  $p = 0.5664$ ; sS,  $F(3,2509) = 0.9200$ ,  $p = 0.4303$ ) (Figures 5A and 5B). Collectively, although there are consistent differences in baseline levels between control and lesioned animals, the performance of lesioned rats is modulated by the number of preceding trials, as it is in controls.

We also examined whether these behavioral measures changed as a consequence of sequence interruption (i.e., when a STOP trial interrupts a string of GOs [sG] or vice versa [gS]). For sG trials, we observed significant main effects of treatment ( $F(3,2718) = 61.53$ ,  $p < 0.0001$ ) and number of preceding STOPs ( $F(3,2718) = 15.36$ ,  $p < 0.0001$ ), as well as a significant interaction

(treatment  $\times$  number of preceding STOPS) ( $F(3,2718) = 7.780$ ,  $p < 0.0001$ ) (Figure 5C). Similarly, for gS trials, we saw a significant main effect of treatment ( $F(1,3619) = 74.41$ ,  $p < 0.0001$ ), but no significant main effect of the number of preceding GO trials ( $F(4,3619) = 2.234$ ,  $p = 0.0629$ ), nor a significant interaction ( $F(4,3619) = 0.2785$ ,  $p = 0.8920$ ) (Figure 5D). Across these four sets of analyses, we see that unilateral mPFC lesions leave the effects of priming and behavioral adaption largely unimpaired, suggesting that deficits are due to a lack to drive to initiate an action rather than a deficit in representations of task structure or rules.

## DISCUSSION

Collectively, the findings presented here identify a role for mPFC in initiating behavior, as well as disambiguate the role of mPFC from the other frontal areas such as ACC. Previously, we have shown that mPFC activity increases on STOP trials over GO trials; however, in that same paper, we showed that directional selectivity in mPFC was also correlated with movement speed and accuracy on GO trials and the strength of the directional signal was not different between GO and STOP trials.<sup>16</sup> Thus, from these correlates, mPFC appears to contribute to both initiation or inhibition of movement.<sup>7,16</sup> Here, we set out to determine how mPFC contributes to executive control from both a neural and behavioral standpoint as well as to determine if mPFC is functionally distinct from ACC.<sup>17</sup> To do this, we made unilateral lesions to the same region of mPFC that we had previously recorded from in rats performing the same STOP-change task<sup>16</sup> while recording from DMS, a region that receives direct and indirect projections from mPFC and has action selection correlates tied to accurate motor output.<sup>17,30</sup>

We show that although mPFC contributes to driving action initiation, it does not appear to have as strong of a role in redirecting behavior once initiated. In our work, rats with mPFC lesions were worse at GO trials but better at STOP trials, presumably because rats were less sensitive to the onset of the first cue. Importantly, this behavioral pattern caused by mPFC lesions is in contrast with our recent work that showed ACC lesions disrupt STOP trial performance but left GO trial performance unchanged.<sup>17</sup> At the neural level, ACC lesions did not alter processing of the first cue, and instead, ACC lesioned rats showed delayed processing of the STOP cue. Moreover, in ACC lesioned rats, processing in DMS was still weaker during the response epoch,<sup>17</sup> whereas in our mPFC lesioned rats, processing during the response epoch was actually stronger. These different patterns of behavioral and neural firing associated with mPFC and ACC, respectively, are striking because in both cases, we recorded from the exact same region of DMS in rats performing the exact same task, although importantly, in both experiments, we did not explicitly examine direct projections from either region to DMS.

Taken together, these findings offer a physiological and functional dissociation of the roles of mPFC and ACC in rats performing the same task. Importantly, although we acknowledge that there are clear differences between the anatomical connectivity of rodent, primate, and human medial frontal cortices,<sup>13,42,43</sup> these observations suggest that despite the debate over homology,<sup>13,44</sup> our ACC<sup>17</sup> and mPFC lesions clearly delineate functionally distinct areas in the rat frontal lobe that largely map on the functional distinctions described in humans.<sup>13,42,44,45</sup> Further, these findings

suggest that rat mPFC and ACC both modulate DMS during stop-change performance and suggest a neural circuit, whereby mPFC is tasked with initiating and driving appropriate action selection, and ACC is responsible for detecting when sensory inputs differ from the intended motor output. Future work should examine how DMS integrates both pieces of information as well as explore these functional and physiological differences using alternative methods such as optogenetics. There is great value in lesion-based approaches, and in some ways, lesions better mimic patient populations with brain-damage;<sup>31</sup> however, transient manipulations such as optogenetics could target these circuits more directly and with greater precision, which may allow for better investigation of the role that timing plays in modulating action selection.<sup>46–48</sup>

In some aspects, our results are consistent with work suggesting that mPFC is important for action initiation in the context of goal-directed behavior<sup>49–53</sup> and that blocking dopamine receptors in mPFC prolongs reaction times on GO trials.<sup>54</sup> Our work offers a potential explanation for these findings, by showing that disruption of mPFC impairs sensitivity to the first cue, both behaviorally and in DMS. Consistent with this hypothesis, mPFC lesioned rats exhibited a significant but weaker speed-accuracy tradeoff (Figure S1i).<sup>55</sup> This fits with work suggesting that mPFC is important for decision-making and may modulate response vigor.<sup>56,57</sup> Although our results are consistent with work suggesting that mPFC is important for action selection, others have reported no changes in GO accuracy or reaction times.<sup>54,58</sup> Our finding that mPFC does not contribute to STOP-change performance is at odds with work showing that mPFC lesions produce minimal behavioral differences on STOP trials<sup>58</sup> and that muscimol inactivation of mPFC increases the SSRT and reduces STOP accuracy.<sup>54</sup>

These discrepancies are likely due to a couple of factors. First, our lesions are unilateral, which only produce relatively mild impairments in behavior (~5%–10%), allowing us to examine neural firing in animals without severe behavioral deficits. Second, our rats are trained over many months on a more complex STOP-change task with two directions. Overtraining, may have more permanently entrained the mPFC and connected regions to handle the basic structure of the task, allowing us to probe key functions lost after a less severe perturbation. The nature of the task may also more strongly engages spatial attention and other cognitive/executive control mechanisms not present in other paradigms, thus increasing the need for mPFC during GO trials. Finally, in our task, rats do not simply STOP, they must redirect, which may engage other systems and/ or mask STOP effects due to attenuated GO initiation. Previous pharmacological<sup>26</sup> and chemogenetic<sup>27–29</sup> dissections of projecting neurons from mPFC to DMS have revealed a clear role for this circuit in cue-driven goal-directed behavior, and we believe that future work using our task in combination with these techniques is needed.

Still, others have shown mPFC inactivation increases premature responding by training rats to first initiate and hold a lever press for a specific time period.<sup>8,24</sup> Because the researchers measured premature responding after action initiation, comparison with the work presented here is difficult but suggests mPFC activity may be modulated by initial task engagement suggesting some consistency with these studies. Our work also fits in part with recent theoretical work suggesting a role for mPFC in

modulating action selection in DMS.<sup>5</sup> In this model, DMS is tasked with maintaining a state transition matrix that offers a readout of possible behaviors based on the confines of the task. Researchers propose that mPFC is in turn tasked with helping DMS form these transition matrices and in providing top-down control to help DMS determine which matrix should be active.<sup>5</sup> Consistent with this proposed role for mPFC, mPFC lesioned rats were slower to initiate actions suggestive of a deficit in the formation and/or correct implementation of the appropriate transition matrix. This is further supported by our population and single unit recording data from DMS, showing that in controls, population and single unit data support the formation of clear intended actions, but in mPFC lesioned rats, encoding for the first cue by DMS did not emerge, suggesting a general slowing or a lack of drive with regards to behavior.

In summary, we performed unilateral excitotoxic lesions of mPFC in rats performing a novel-variant of the stop-signal task while recording downstream of the same hemisphere of DMS. At both the behavioral and neural levels, we show that lesions to mPFC alter the ability of rats and DMS neurons to appropriately respond to the first cue, thereby delaying initiation of the action. Analysis of the effect of trial history suggests that although baseline behavioral differences exist, mPFC lesioned rats are capable of adapting behavior similar to controls. Collectively, the data suggest that mPFC contributes to the drive to initiate movements in response to spatial visual stimuli in the context of our stop-change task.

## STAR★METHODS

Detailed methods are provided in the online version of this paper and include the following:

- KEY RESOURCES TABLE
- RESOURCE AVAILABILITY
  - Lead contact
  - Materials availability
  - Data and code availability
- EXPERIMENTAL MODEL AND SUBJECT DETAILS
- METHOD DETAILS
  - Stop-change Task
  - Ibotenic Acid Injection
  - Electrode Implantation
  - Single-Unit Recordings
  - Histology
- QUANTIFICATION AND STATISTICAL ANALYSIS
  - Behavioral analysis
  - Population histograms, single units, and waveform analysis

## SUPPLEMENTAL INFORMATION

Supplemental information can be found online at <https://doi.org/10.1016/j.cub.2022.06.025>.

## ACKNOWLEDGMENTS

The authors would also like to thank their funding sources for their support in conducting this work: NIMH (MH1117836 to A.T.B.) and NIDA (DA031695 to M.R.R.).

## AUTHOR CONTRIBUTIONS

A.T.B. and M.R.R. conceived of, designed, analyzed, wrote, and edited the text. A.T.B., S.S.T., C.A.D., and M.K. carried out data collection. S.S.T., C.A.D., and M.K. edited the final text.

## DECLARATION OF INTERESTS

The authors declare no competing interests.

Received: December 8, 2021

Revised: March 6, 2022

Accepted: June 9, 2022

Published: July 7, 2022

## REFERENCES

1. Miller, E.K. (2000). The prefrontal cortex and cognitive control. *Nat. Rev. Neurosci.* *1*, 59–65.
2. Botvinick, M.M., Braver, T.S., Barch, D.M., Carter, C.S., and Cohen, J.D. (2001). Conflict monitoring and cognitive control. *Psychol. Rev.* *108*, 624–652.
3. Miller, E.K., and Cohen, J.D. (2001). An integrative theory of prefrontal cortex function. *Annu. Rev. Neurosci.* *24*, 167–202.
4. Braver, T.S., and Barch, D.M. (2002). A theory of cognitive control, aging cognition, and neuromodulation. *Neurosci. Biobehav. Rev.* *26*, 809–817.
5. Sharpe, M.J., Stalnaker, T., Schuck, N.W., Killcross, S., Schoenbaum, G., and Niv, Y. (2019). An integrated model of action selection: distinct modes of cortical control of striatal decision making. *Annu. Rev. Psychol.* *70*, 53–76.
6. Brockett, A.T., and Roesch, M.R. (2021). Anterior cingulate cortex and adaptive control of brain and behavior. *Int. Rev. Neurobiol.* *158*, 283–309.
7. Brockett, A.T., and Roesch, M.R. (2021). Reactive and proactive adaptation of cognitive and motor neural signals during performance of a stop-change task. *Brain Sci* *11*, 617.
8. Narayanan, N.S., Horst, N.K., and Laubach, M. (2006). Reversible inactivations of rat medial prefrontal cortex impair the ability to wait for a stimulus. *Neuroscience* *139*, 865–876.
9. Narayanan, N.S., Cavanagh, J.F., Frank, M.J., and Laubach, M. (2013). Common medial frontal mechanisms of adaptive control in humans and rodents. *Nat. Neurosci.* *16*, 1888–1895.
10. Schmidt, R., Leventhal, D.K., Mallet, N., Chen, F., and Berke, J.D. (2013). Canceling actions involves a race between basal ganglia pathways. *Nat. Neurosci.* *16*, 1118–1124.
11. Wessel, J.R., and Aron, A.R. (2017). On the globality of motor suppression: unexpected events and their influence on behavior and cognition. *Neuron* *93*, 259–280.
12. Narayanan, N.S., and Laubach, M. (2006). Top-down control of motor cortex ensembles by dorsomedial prefrontal cortex. *Neuron* *52*, 921–931.
13. Laubach, M., Amarante, L.M., Swanson, K., and White, S.R. (2018). What, if anything, is rodent prefrontal cortex? *eNeuro* *5*, ENEURO.0315-0318.2018.
14. Verbruggen, F., Aron, A.R., Band, G.P., Beste, C., Bissett, P.G., Brockett, A.T., Brown, J.W., Chamberlain, S.R., Chambers, C.D., Colonius, H., et al. Poldrack, R.A., Ridderinkhof, K.R., Robbins, T.W., Roesch, M., Rubia, K., Schachar, R.J., Schall, J.D., Stock, A.K., Swann, N.C., Thakkar, K.N., van der Molen, M.W., Vermeylen, L., Vink, M., Wessel, J.R., Whelan, R., Zandbelt, B.B., Boehler, C.N. (2019). A consensus guide to capturing the ability to inhibit actions and impulsive behaviors in the stop-signal task. *eLife* *8*, e46323.
15. Bryden, D.W., Brockett, A.T., Blume, E., Heatley, K., Zhao, A., and Roesch, M.R. (2019). Single neurons in anterior cingulate cortex signal the need to change action during performance of a stop-change task that induces response competition. *Cereb. Cortex* *29*, 1020–1031.

16. Bryden, D.W., Burton, A.C., Barnett, B.R., Cohen, V.J., Hearn, T.N., Jones, E.A., Kariyil, R.J., Kunin, A., Kwak, S.I., Lee, J., et al. (2016). Prenatal nicotine exposure impairs executive control signals in medial prefrontal cortex. *Neuropsychopharmacology* *41*, 716–725.
17. Brockett, A.T., Tennyson, S.S., deBettencourt, C.A., Gaye, F., and Roesch, M.R. (2020). Anterior cingulate cortex is necessary for adaptation of action plans. *Proc. Natl. Acad. Sci. USA* *117*, 6196–6204.
18. Shenhav, A., Cohen, J.D., and Botvinick, M.M. (2016). Dorsal anterior cingulate cortex and the value of control. *Nat. Neurosci.* *19*, 1286–1291.
19. Haddon, J.E., and Killcross, S. (2006). Prefrontal cortex lesions disrupt the contextual control of response conflict. *J. Neurosci.* *26*, 2933–2940.
20. Marquis, J.-P., Killcross, S., and Haddon, J.E. (2007). Inactivation of the prelimbic, but not infralimbic, prefrontal cortex impairs the contextual control of response conflict in rats. *Eur. J. Neurosci.* *25*, 559–566.
21. Brockett, A.T., Kane, G.A., Monari, P.K., Briones, B.A., Vigneron, P.-A., Barber, G.A., Bermudez, A., Dieffenbach, U., Kloth, A.D., Buschman, T.J., and Gould, E. (2018). Evidence supporting a role for astrocytes in the regulation of cognitive flexibility and neuronal oscillations through the Ca<sup>2+</sup> binding protein S100 $\beta$ . *PLoS One* *13*, e0195726.
22. Brockett, A.T., LaMarca, E.A., and Gould, E. (2015). Physical exercise enhances cognitive flexibility as well as astrocytic and synaptic markers in the medial prefrontal cortex. *PLoS One* *10*, e0124859.
23. Birrell, J.M., and Brown, V.J. (2000). Medial frontal cortex mediates perceptual attentional set shifting in the rat. *J. Neurosci.* *20*, 4320–4324.
24. Risterucci, C., Terramorsi, D., Nieoullon, A., and Amalric, M. (2003). Excitotoxic lesions of the prelimbic-infralimbic areas of the rodent prefrontal cortex disrupt motor preparatory processes. *Eur. J. Neurosci.* *17*, 1498–1508.
25. Broersen, L.M., and Uylings, H.B. (1999). Visual attention task performance in Wistar and Lister hooded rats: response inhibition deficits after medial prefrontal cortex lesions. *Neuroscience* *94*, 47–57.
26. Baker, P.M., and Ragozzino, M.E. (2014). Contralateral disconnection of the rat prelimbic cortex and dorsomedial striatum impairs cue-guided behavioral switching. *Learn. Mem.* *21*, 368–379.
27. Shipman, M.L., Johnson, G.C., Bouton, M.E., and Green, J.T. (2019). Chemogenetic silencing of prelimbic cortex to anterior dorsomedial striatum projection attenuates operant responding. *eNeuro* *6*. ENEURO.0125-19.2019.
28. Hart, G., Bradfield, L.A., Fok, S.Y., Chieng, B., and Balleine, B.W. (2018). The bilateral prefronto-striatal pathway is necessary for learning new goal-directed actions. *Curr. Biol.* *28*, 2218–2229. e7.
29. Terra, H., Bruinsma, B., de Kloet, S.F., van der Roest, M., Pattij, T., and Mansvellder, H.D. (2020). Prefrontal cortical projection neurons targeting dorsomedial striatum control behavioral inhibition. *Curr. Biol.* *30*, 4188–4200. e5.
30. Bryden, D.W., Burton, A.C., Kashtelyan, V., Barnett, B.R., and Roesch, M.R. (2012). Response inhibition signals and miscoding of direction in dorsomedial striatum. *Front. Integr. Neurosci.* *6*, 69.
31. Vaidya, A.R., Pujara, M.S., Petrides, M., Murray, E.A., and Fellows, L.K. (2019). Lesion studies in contemporary neuroscience. *Trends Cogn. Sci.* *23*, 653–671.
32. Lomber, S.G. (1999). The advantages and limitations of permanent or reversible deactivation techniques in the assessment of neural function. *J. Neurosci. Methods* *86*, 109–117.
33. Martin, J.H., and Ghez, C. (1999). Pharmacological inactivation in the analysis of the central control of movement. *J. Neurosci. Methods* *86*, 145–159.
34. Bryden, D.W., and Roesch, M.R. (2015). Executive control signals in orbitofrontal cortex during response inhibition. *J. Neurosci.* *35*, 3903–3914.
35. Brockett, A.T., Hricz, N.W., Tennyson, S.S., Bryden, D.W., and Roesch, M.R. (2020). Neural signals in red nucleus during reactive and proactive adjustments in behavior. *J. Neurosci.* *40*, 4715–4726.
36. Tennyson, S.S., Brockett, A.T., Hricz, N.W., Bryden, D.W., and Roesch, M.R. (2018). Firing of putative dopamine neurons in ventral tegmental area is modulated by probability of success during performance of a stop-change task. *eNeuro* *5*. ENEURO.0007-18, 2018.
37. Vandaele, Y., Ottenheimer, D.J., and Janak, P.H. (2021). Dorsomedial striatal activity tracks completion of behavioral sequences in rats. *eNeuro* *8*. ENEURO.0279-21, 2021.
38. Mueller, L.E., Sharpe, M.J., Stalnaker, T.A., Wikenheiser, A.M., and Schoenbaum, G. (2021). Prior cocaine use alters the normal evolution of information coding in striatal ensembles during value-guided decision-making. *J. Neurosci.* *41*, 342–353.
39. Berke, J.D. (2008). Uncoordinated firing rate changes of striatal fast-spiking interneurons during behavioral task performance. *J. Neurosci.* *28*, 10075–10080.
40. Brockett, A.T., and Roesch, M.R. (2021). The ever-changing OFC landscape: what neural signals in OFC can tell us about inhibitory control. *Behav. Neurosci.* *135*, 129–137.
41. Brockett, A.T., Vázquez, D., and Roesch, M.R. (2021). Prediction errors and valence: from single units to multidimensional encoding in the amygdala. *Behav. Brain Res.* *404*, 113176.
42. Wise, S.P. (2008). Forward frontal fields: phylogeny and fundamental function. *Trends Neurosci* *31*, 599–608.
43. Schaeffer, D.J., Hori, Y., Gilbert, K.M., Gati, J.S., Menon, R.S., and Everling, S. (2020). Divergence of rodent and primate medial frontal cortex functional connectivity. *Proc. Natl. Acad. Sci. USA* *117*, 21681–21689.
44. Heilbronner, S.R., Rodriguez-Romaguera, J., Quirk, G.J., Groenewegen, H.J., and Haber, S.N. (2016). Circuit-based corticostriatal homologies between rat and primate. *Biol. Psychiatry* *80*, 509–521.
45. Brown, V.J., and Bowman, E.M. (2002). Rodent models of prefrontal cortical function. *Trends Neurosci* *25*, 340–343.
46. Emmons, E.B., De Corte, B.J., Kim, Y., Parker, K.L., Matell, M.S., and Narayanan, N.S. (2017). Rodent medial frontal control of temporal processing in the dorsomedial striatum. *J. Neurosci.* *37*, 8718–8733.
47. Bakhurin, K.I., Goudar, V., Shobe, J.L., Claar, L.D., Buonomano, D.V., and Masmanidis, S.C. (2017). Differential encoding of time by prefrontal and striatal network dynamics. *J. Neurosci.* *37*, 854–870.
48. Wang, J., Narain, D., Hosseini, E.A., and Jazayeri, M. (2018). Flexible timing by temporal scaling of cortical responses. *Nat. Neurosci.* *21*, 102–110.
49. Ostlund, S.B., and Balleine, B.W. (2005). Lesions of medial prefrontal cortex disrupt the acquisition but not the expression of goal-directed learning. *J. Neurosci.* *25*, 7763–7770.
50. Capuzzo, G., and Floresco, S.B. (2020). Prelimbic and infralimbic prefrontal regulation of active and inhibitory avoidance and reward-seeking. *J. Neurosci.* *40*, 4773–4787.
51. Jodo, E., Suzuki, Y., and Kayama, Y. (2000). Selective responsiveness of medial prefrontal cortex neurons to the meaningful stimulus with a low probability of occurrence in rats. *Brain Res* *856*, 68–74.
52. Ishikawa, A., Ambroggi, F., Nicola, S.M., and Fields, H.L. (2008). Contributions of the amygdala and medial prefrontal cortex to incentive cue responding. *Neuroscience* *155*, 573–584.
53. Ishikawa, A., Ambroggi, F., Nicola, S.M., and Fields, H.L. (2008). Dorsomedial prefrontal cortex contribution to behavioral and nucleus accumbens neuronal responses to incentive cues. *J. Neurosci.* *28*, 5088–5098.
54. Bari, A., Mar, A.C., Theobald, D.E., Elands, S.A., Oganya, K.C.N.A., Eagle, D.M., and Robbins, T.W. (2011). Prefrontal and monoaminergic contributions to stop-signal task performance in rats. *J. Neurosci.* *31*, 9254–9263.
55. Small, D.M., Gitelman, D.R., Gregory, M.D., Nobre, A.C., Parrish, T.B., and Mesulam, M.-M. (2003). The posterior cingulate and medial prefrontal cortex mediate the anticipatory allocation of spatial attention. *NeuroImage* *18*, 633–641.
56. Amarante, L.M., and Laubach, M. (2021). Coherent theta activity in the medial and orbital frontal cortices encodes reward value. *eLife* *10*, e63372.

57. Amarante, L.M., Caetano, M.S., and Laubach, M. (2017). Medial frontal theta is entrained to rewarded actions. *J. Neurosci.* *37*, 10757–10769.
58. Eagle, D.M., and Robbins, T.W. (2003). Lesions of the medial prefrontal cortex or nucleus accumbens core do not impair inhibitory control in rats performing a stop-signal reaction time task. *Behav. Brain Res.* *146*, 131–144.
59. National Research Council (US) Committee for the Update of the Guide for the Care and Use of Laboratory Animals (2011). *Guide for the Care and Use of Laboratory Animals*, Eighth Edition (National Academies Press).
60. Bryden, D.W., Johnson, E.E., Tobia, S.C., Kashtelyan, V., and Roesch, M.R. (2011). Attention for learning signals in anterior cingulate cortex. *J. Neurosci.* *31*, 18266–18274.
61. Verbruggen, F., and Logan, G.D. (2008). Response inhibition in the stop-signal paradigm. *Trends Cogn. Sci.* *12*, 418–424.
62. Kashtelyan, V., Tobia, S.C., Burton, A.C., Bryden, D.W., and Roesch, M.R. (2012). Basolateral amygdala encodes upcoming errors but not response conflict. *Eur. J. Neurosci.* *35*, 952–959.



## STAR★METHODS

## KEY RESOURCES TABLE

REAGENT or RESOURCE	SOURCE	IDENTIFIER
Chemicals, peptides, and recombinant proteins		
Chloroplatinic acid solution (H <sub>2</sub> PtCl <sub>6</sub> )	Sigma- Aldrich	<a href="https://www.sigmaaldrich.com/US/en/product/aldrich/262587?amp;region=US">https://www.sigmaaldrich.com/US/en/product/aldrich/262587?amp;region=US</a>
Cresyl violet acetate	Sigma-Aldrich	<a href="https://www.sigmaaldrich.com/US/en/product/sigma/c5042">https://www.sigmaaldrich.com/US/en/product/sigma/c5042</a>
Ibotenic acid	ABCam	<a href="https://www.abcam.com/ibotenic-acid-excitotoxic-agonist-ab120041.html">https://www.abcam.com/ibotenic-acid-excitotoxic-agonist-ab120041.html</a>
Deposited data		
Dataset	DRUM	<a href="http://hdl.handle.net/1903/28599">http://hdl.handle.net/1903/28599</a>
Experimental models: Organisms/strains		
Rat; Long-Evans	Charles River Laboratory	<a href="https://www.criver.com/products-services/find-model/long-evans-rat?region=3611">https://www.criver.com/products-services/find-model/long-evans-rat?region=3611</a>
Software and algorithms		
GraphPad Prism 9	GraphPad Software	<a href="https://www.graphpad.com/">https://www.graphpad.com/</a>
Matlab 2018a	Mathworks	<a href="https://www.mathworks.com/products/matlab.html">https://www.mathworks.com/products/matlab.html</a>
Neuroexplorer	Plexon	<a href="https://plexon.com/products/neuroexplorer/">https://plexon.com/products/neuroexplorer/</a>
Offline Sorter V3	Plexon	<a href="https://plexon.com/products/offline-sorter/">https://plexon.com/products/offline-sorter/</a>

## RESOURCE AVAILABILITY

## Lead contact

Further information and requests for resources should be directed to and will be fulfilled by the lead contact, Dr. Matthew Roesch ([mroesch@umd.edu](mailto:mroesch@umd.edu))

## Materials availability

This study did not generate new unique reagents.

## Data and code availability

Data is publicly available at the following link: <http://hdl.handle.net/1903/28599>. For questions regarding the data or analysis code please contact: Dr. Matthew Roesch ([mroesch@umd.edu](mailto:mroesch@umd.edu)).

## EXPERIMENTAL MODEL AND SUBJECT DETAILS

5 female and 8 male Long-Evans rats ( $n = 13$ ) were obtained at 175–200 g from Charles River Laboratories, and weighed an average of  $306.8 \pm 34.59$  g (females) and  $488.6 \pm 32.30$  g (males) at the time of surgery. Rats were housed on a 12/12 h light/dark schedule with lights on at 6:00 am EST. All training, behavioral testing, and recordings occurred between 6:00 am and 2:00 pm EST. Food was provided *ad libitum*, but rats were water restricted throughout training and testing. Water was provided for approximately 20 minutes each day of training/ testing after rats had completed the day's session. All experimental procedures were approved by the University of Maryland Animal Care and Use Committee and conformed to the guidelines set forth by the National Research Council.<sup>59</sup>

## METHOD DETAILS

## Stop-change Task

The task design is illustrated in Figure 1A. Each trial began with illumination of a house light that instructed the rat to nose poke into a central port. Nose poking initiated a 1000 ms pre-cue delay period. At the end of this delay, a directional light to the rat's left or right was flashed for 100 ms. If the rat exited the port at any time before offset of the directional cue light, the trial was aborted and house lights were extinguished. On 80% of trials (GO trials), presentation of the left or right light signaled the direction in which the rat should respond in order to obtain a 10% sucrose solution reward in the corresponding fluid well below. On the remaining 20% of trials (STOP trials), the light opposite to the location of the originally cued direction turned on either at the same time as port exit or after a randomly

selected stop-signal delay (0–100 ms) and remained illuminated until the behavioral response was made. On STOP trials, rats were required to inhibit the movement signaled by the first light and respond in the direction of the second light. GO and STOP trials were randomly interleaved. On correct responding trials, rats were required to remain in the fluid well for a variable period between 800–1000 ms (pre-fluid delay) before reward delivery (10% liquid sucrose solution). Error trials (incorrect direction) were immediately followed by the extinction of house lights and ITI onset of 4 s.

Trials were presented in a pseudorandom sequence such that left and right trials were presented in roughly equal numbers. The time necessary to stop and redirect a motor action (stop-change reaction time [SCRT]) on STOP trials was computed using the difference between the average movement time on correct STOP and GO trials.<sup>6,7,15–17,30,34,36,60</sup> While we recognize there are multiple ways to estimate the timing necessary to inhibit a movement,<sup>61</sup> we choose to use SCRT because we have access to STOP trial movement time distributions and we vary the stop-signal delay systematically across sessions, making SSRT-mean and integration methods inappropriate for our dataset.<sup>14,61</sup>

### Ibotenic Acid Injection

All surgical procedures were conducted using aseptic technique. Rats (5F, 8M) were randomly assigned to either the saline (3F, 4M) or ibotenic acid (2F, 4M) treatment conditions prior to surgery. Behavioral performance during training was assessed for the last five days of training prior to surgery in order to verify that groups showed no difference in behavioral performance prior to surgery. Rats, regardless of treatment condition, received two unilateral stereotaxic injections spaced 1 mm apart targeting the prelimbic portion of mPFC at the following coordinates relative to bregma (Injection 1: Anterior-Posterior: +3.5 mm; Medial-Lateral: ±0.6 mm; Dorsal-Ventral: -4.0 mm; Injection 2: Anterior-Posterior: +2.5 mm; Medial-Lateral: ±0.6 mm; Dorsal-Ventral: -3.8 mm). Coordinates were chosen based on a previous recording study targeting the same area.<sup>16</sup> For each injection site a beveled 33 ga 5 μl Hamilton Neuros Syringe (Hamilton) was lowered slowly over the course of five minutes to its final depth. Care was taken to insure the bevel of the needle was positioned away from the midline of the brain. Rats were unilaterally infused with either 0.2 μl of 0.6M ibotenic acid in saline or 0.2 μl of 0.9% sterile saline per injection site over the course of 3 minutes (approximately: 125 nl/ minute). Needles were left in place for 5 minutes before being slowly removed over the course of an additional 5 minutes in order to minimize tissue damage and backflow. Holes were loosely packed with sterile bonewax prior to beginning electrode implantation.

### Electrode Implantation

Electrodes were implanted unilaterally in DMS in the same hemisphere of the brain that had received the two stereotaxic injections of either saline or ibotenic acid. Brain hemispheres were counterbalanced across groups and the methods for implantation have been described in detail previously.<sup>15–17,30,34,36,60,62</sup> Rats were chronically implanted with a drivable bundle of ten 25 μm diameter FeNiCr wires (Stablohm 675, California Fine Wire, Grover Beach, CA) into either the left or right hemisphere of DMS using the following coordinates relative to bregma (Anterior-Posterior: -0.4 mm; Medial-Lateral: ±2.4 mm; Dorsal-Ventral: -3.5 mm). Coordinates were chosen based on our previous results investigating the role of DMS using the stop-change task.<sup>17,30</sup> Immediately prior to implantation, wires were freshly cut with surgical scissors to extend ~1 mm beyond the cannula and were electroplated with platinum (H<sub>2</sub>Cl<sub>6</sub>Pt) to an impedance of ~300kOhms. Immediately, following surgery, rats were administered Rimadyl (5mg/kg) subcutaneously and the skin surrounding the surgical site was treated topically with a mixture of lidocaine and Neosporin. Rats also received subcutaneous injections of Rimadyl (5mg/kg) once daily for 2–3 days, and Cephalexin (15 mg kg<sup>-1</sup>) was administered orally twice per day for seven days following surgery.

### Single-Unit Recordings

Procedures for single unit recordings in rats performing the stop-change task are the same as those described previously.<sup>15–17,30,34,36,60</sup> Briefly, wires were screened for activity daily; if no activity was detected, the rat was removed and the electrode assembly was advanced 40 or 80 μm. If activity was detected, rats then performed the day's session, and the electrode assembly was advanced at the end of the session. Neural activity was recorded using four identical Plexon Multichannel Acquisition Processor Systems. Signals from electrode wires were amplified 20x by an op-amp headstage located on the electrode array. Immediately outside the training chamber, signals were passed through a differential pre-amplifier (Plexon, PBX2/16sp-r-G50/16fp-G50), where single unit signals were amplified 50x and filtered at 150–9000 Hz. The single unit signals were then sent to the Multichannel Acquisition Processor box, where they were further filtered at 250–8000 Hz, digitized at 40 kHz and amplified at 1–32x. Waveforms (>2.5:1 signal-to-noise) were extracted from active channels and recorded to disk by an associated workstation with event timestamps from the behavior computer.

### Histology

Following the completion of testing, rats were overdosed with isoflurane and a transcardial perfusion was performed using 4% paraformaldehyde (PFA). Following perfusion, the electrode assembly was removed slowly from the skull and brains were extracted. Brains were post-fixed for 48 hours in 4% PFA, before being moved to a 30% sucrose solution for cryoprotection. Following cryoprotection, brains were then blocked, flash frozen in alcohol, and sectioned on a freezing microtome. 40 μm coronal sections were cut throughout mPFC and DMS. Sections were collected, mounted to positively charged Superfrost slides and Nissl stained. Slides were viewed under a light microscope and the size of the lesion and presence or absence of electrode tracks were

verified and cross-referenced with score sheets demarcating electrode assembly advancement. Traces of the lesion and electrode track were made onto coordinate matched printouts of stereotaxic space.

### QUANTIFICATION AND STATISTICAL ANALYSIS

We recorded a total of 749 units (Control:  $n = 465$  [123, 102, 119, 55, 37, 15, 14]; Lesion  $n = 284$  [86, 75, 38, 30, 28, 27]). Units were sorted offline via Offline Sorter Version 3.3 software (Plexon) using a template matching algorithm and analyzed using Neuroexplorer Version 4 software (Plexon) and Matlab (Mathworks; Natick, MA; 2018b). Activity was examined during two main epochs. The “cue epoch” consisted of the 400 ms after onset of the first cue. The second epoch encompassed time from port exit to well entry, which we refer to as the “response epoch”. Note that there was no overlap between the two epochs.

#### Behavioral analysis

Unless otherwise specified, behavioral data was analyzed using a two-way ANOVA where each data point represents a session average. To capture activity that differentiated based on previous trial we examined firing rates on GO and STOP trials that followed either a GO or STOP trial. This analysis allows for the examination of sequence effects as well as comparisons between trials that were not preceded by a need to adapt behavior (i.e., when a STOP follows a GO) versus trials that were preceded by a need to adapt behavior (i.e., when a STOP follows a STOP). Abbreviation for these trials are differentiated by the trial type preceding it being denoted as lowercase (i.e., ‘g’ or ‘s’: ‘GO’ or ‘STOP’).

#### Population histograms, single units, and waveform analysis

Units were classified as putative tonically active neurons (TANs), fast-spiking interneurons (FSIs), or putative medium spiny neurons (MSNs) based on their respective waveforms.<sup>30,37–39</sup> Putative TANs were defined by a half-valley width greater than 0.45 ms, and a baseline firing rate lower than 5 Hz (Control: 0.2%; Lesions: 0.4%). Putative FSIs were defined by a half-valley width lower than 0.15 ms and a baseline firing rate higher than 20 Hz (Control: 4.08%; Lesion: 2.46%). Units with a half-valley width between 0.15 and 0.45 and a firing rate between 5 and 20 Hz were classified as putative MSNs, and relative ratios of TANs:FSIs:MSNs were consistent with previous work.<sup>30,37–39</sup> Activity in the population histograms was normalized by dividing by the maximal firing rate of each neuron, and smoothed using a box-car smoothing method that averaged the current 100ms time bin by the 100ms time bins before and after. For analysis of single units, we computed distributions of difference scores based on the raw firing rate (spikes/s) for each neuron. Distributions were deemed significant if they differed from either zero or one another via Wilcoxon sign-rank and rank sum, respectively. To determine the percentage of selective neurons on gG and sG trials across trial-time, a sliding Wilcoxon test across 100ms bins comparing firing between preferred and non-preferred directions was conducted, then the total number of significant cells were tallied and divided by the total number of cells. Chi-square tests were performed for each bin comparing the percentage of selective cells for control versus lesioned rats. With the exception of the error analysis in [Figure 4](#), unless otherwise stated, all analyses were performed on correctly performed trials.